Microchimica Acta (2019) 186:568
https://doi.org/10.1007/s00604-019-3675-3

ORIGINAL PAPER

Sensitive fluorometric determination of glutathione using fluorescent polymer dots and the dopamine-melanin nanosystem

Jing Wang[1] · Cheng Zheng[2] · Xionghong Tan[3,4] · Aixian Zheng[3,4] · Yongyi Zeng[3,4,5] · Zhenxi Zhang[1] · Xiaolong Zhang[3,4] · Xiaolong Liu[1,3,4]

Received: 22 March 2019 / Accepted: 6 July 2019

Abstract

A bioinspired fluorometric method has been developed for the detection of glutathione (GSH) in biological fluids. It is based on the use of near-infrared fluorescent semiconducting polymer dots (P-dots) and of the dopamine (DA)-melanin nanosystem. The P-dots were prepared from poly(styrene-co-maleic anhydride), the semiconducting polymer poly[(9,9′-dioctyl-2,7-divinylenefluorenylene)-alt-2-methoxy-5-(2-ethyl-hexyloxy)-1,4-phenylene] and the fluorescent dye tetraphenylporphyrin. They have excitation/emission maxima at 458/656 nm, and this enables measurement to be performed with low autofluorescence and scattering background. DA can self-polymerize on the surface of the P-dots to yield a poly-DA coating. This coating, at weak alkaline pH values, causes the quenching of the fluorescence of the P-dots. However, the polymerization of DA is inhibited by GSH. Hence, quenching of fluorescence is prevented. This effect was used to design a fluorometric assay for GSH that has good selectivity and sensitivity. Under optimal conditions, the method has a linear response in the 0.2 to 20 μM GSH concentration range and a 60 nM detection limit. It was successfully applied to the determination of GSH in HepG2 cells and in spiked human serum.

Keywords Polydopamine · Semiconducting polymer dots · Antiquenching · Antioxidant · PEPV · Biothiols · Tetraphenylporphyrin · Cell extracts · Serum · Nanoparticles

Introduction

Glutathione (GSH) is the most abundant and important intracellular nonprotein biothiol and plays a crucial role in biological functions. [1–3] The imbalance of GSH homeostasis is concerned with various clinical diseases, such as liver or lung damage, cancer, AIDS, Alzheimer's and Parkinson's disease. [4–7] Therefore, analysis of GSH in biological samples is of continuous interest and great significance in biomedical applications.

Various methods have been developed for determination of GSH in biological samples, such as chromatography, [8] electrochemical, [9] colorimetric, [10–12] electrochemiluminescence (ECL), [13] surface-enhanced

Jing Wang and Cheng Zheng contributed equally to this work.

Electronic supplementary material The online version of this article (https://doi.org/10.1007/s00604-019-3675-3) contains supplementary material, which is available to authorized users.

✉ Xiaolong Zhang
xiaolongdo@gmail.com

✉ Xiaolong Liu
xiaoloong.liu@gmail.com

[1] The Key Laboratory of Biomedical Information Engineering of Ministry of Education, School of Life Science and Technology, Xi'an Jiaotong University, Xi'an 710049, People's Republic of China

[2] College of Chemistry, Fuzhou University, Fuzhou 350116, People's Republic of China

[3] The United Innovation of Mengchao Hepatobiliary Technology Key Laboratory of Fujian Province, Mengchao Hepatobiliary Hospital of Fujian Medical University, Fuzhou 350025, People's Republic of China

[4] The Liver Center of Fujian Province, Fujian Medical University, Fuzhou 350025, People's Republic of China

[5] Liver Disease Center, The First Affiliated Hospital of Fujian Medical University, Fuzhou 350005, People's Republic of China

Published online: 24 July 2019

Raman scattering (SERS), [14] and fluorescence methods. [15, 16] Among them, fluorescence method has attracted a lot of attention for its high sensitivity, tunable emissions, ease of operation, and nondestructive properties. [17] So, a series of fluorescent probes have been developed for detection of GSH, such as organic fluorophores, [18] semiconductor quantum dots (QDs), [19] fluorescent metal nanoclusters, [20] carbon nanomaterials, [21] and upconversion nanoparticles (UCNPs). [22] Although their usefulness in GSH fluorescence detection, there are still room for improvement, for example, vulnerable to photobleaching, time-consuming and complex synthesis steps for organic fluorophores; some toxic heavy-metal elements used for QDs or metal nanoclusters based probes; the relatively low quantum yields, high temperature synthesis and overheating effects induced by near-infrared light for UCNPs. Therefore, it is still worthy to explore new fluorescence detection strategies with straightforward, selective, efficient and stable properties for GSH.

The new emerging semiconducting polymer nanoparticles (P-dots) have been developed as a neotype photostable fluorescent nanomaterials. They have outstanding optical properties, such as superior brightness, high emission rates, large Stokes shift and remarkable photostability. [23, 24] The P-dots also show low cytotoxicity, good water dispersibility, facile modification and purification steps. [25] Based on these advantages, they have been developed for chem/bio sensing, molecular imaging and cancer phototherapy. [23–26] When used for sensing platform, the P-dots have been designed for probing oxygen, ions, temperature, reactive oxygen and nitrogen species (RONS) and enzymes. [25] Despite these achievements, there is still of great significance to further expand the application of P-dots in biosensing field.

A bioinspired fluorescence method has been reported for detection of GSH in biological samples based on the NIR fluorescent P-dots and dopamine (DA)-melanin composites. In this approach, the NIR P-dots were used as fluorescent probe and polydopamine (PDA) served as efficient quencher. When in the absence of GSH, the dopamine self-polymerize on P-dots to yield a PDA coating under a weak alkaline buffer condition. This coating leads to the fluorescence quenching of P-dots by nonradiative means of dopamine-melanin. However, in the presence of GSH, the inhibition of dopamine self-polymerization happened. This effect prevented the formation of PDA and fluorescence quenching of P-dots (Fig. 1). The chemical response of GSH showed good selectivity over other compounds. The "antiquenching" effect was related with the concentration range of GSH. In this way, a sensitive, low-cost and selective detection system for GSH was constructed. It was successfully applied for GSH analysis in complex biological samples, such as cell lysates and serum samples.

Experimental section

Reagents and instruments

The fluorescent semiconjugated polymer poly[(9,9′-dioctyl-2,7-divinylene-fluorenylene)-alt-2-methoxy-5-(2-ethyl-hexyloxy)-1,4-phenylene] (PEPV) was purchased from Luminescence Technology Corp (www.lumtec.com.tw). Tetraphenylporphyrin (TPP) was purchased from Adamas-beta (www.adamas-beta.com). Other reagents were listed on Electronic Supporting Material (ESM). Human serum samples were obtained from Mengchao Hepatobiliary Hospital of Fujian Medical University.

UV-vis absorption spectra were tested using a Spectra Max M5 microplate reader (Molecular Devices) in a 1-cm path length quartz cuvette. Fluorescence spectra measurements were collected by using an Cary Eclipse fluorometer (Aglilent, USA). The transmission electron microscopy (TEM) images of the nanomaterials morphology were recorded on JEM-2100F TEM (JEOL, Japan) with an acceleration voltage of 200 kV. Dynamic light scattering (DLS) and zeta potential distribution of P-dots were performed on the Zetasizer Nano-ZS (Malvern, UK).

Preparation of the polymer dots (P-dots)

P-dots were prepared by using a modified reprecipitation method of previously reported works. [27, 28] The details of synthesis can be found in ESM.

Fluorescence quenching of P-dots by polydopamine

To test the fluorescence quenching effect of self-polymerization of DA on fluorescent P-dots, different concentrations of DA solution were added to 200 μL reaction solutions of P-dots (0.4 $mg{\cdot}mL^{-1}$ in Tris-HCl (10 mM, pH = 8.5)) and incubated for a specified time. Subsequently, the UV-vis absorption and fluorescence spectra of the reaction solutions were measured with a 10 min time interval. Also, the corresponding pictures under day-light and UV-light were recorded.

Establishment of the glutathione (GSH) assay

To investigate the antiquenching effects of GSH, 100 μL of various concentrations (0, 0.2, 0.5, 1, 10, 15, 20, 30, 40 μM) of freshly prepared GSH was mixed with 0.4 $mg{\cdot}mL^{-1}$ P-dots before the addition of DA solution (0.75 mM) and then reacted for 30 min at room temperature. The final volume was 200 μL. Thereafter, their fluorescence emission spectra were measured, and the relationship between different concentrations of GSH and fluorescence intensity change was determined by a standard calibration plot. The data were obtained at 458/656 nm as excitation/emission wavelengths.

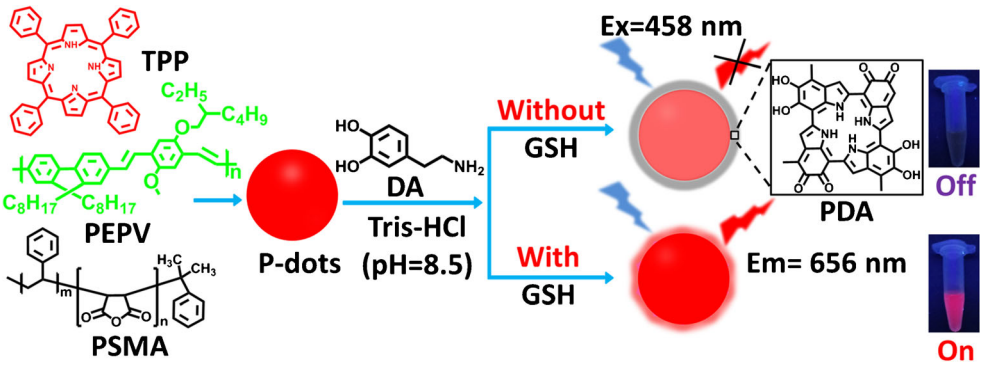

Fig. 1 Schematic illustration of using NIR fluorescent P-dots and dopamine (DA)-melanin nanohybrid system for GSH detection

The selectivity of the GSH assay

To assess the specificity of P-dots and polydopamine (PDA) hybrid system for GSH detection, different non-target interferences were tested, including the metal ions (0.1 mM of K^+, Na^+, Ca^{2+} and Mg^{2+}), amino acids (30 μM of Gly, Leu, Glu), proteins (0.01 mg·mL^{-1} of GOx and 1 mg·mL^{-1} of BSA) and reducing bioagents (1 mg·mL^{-1} Glucose, 30 μM of AA, and Cys). The fluorescence intensity change response to these potential interferences was measured as described above and the corresponding photographs under UV-light was also recorded.

Preparation of cell extracts and determination of GSH in cell extracts

HepG2 cells were cultured in DMEM medium (Invitrogen) supplemented with fetal bovine serum (10% FBS, Gibco), streptomycin/penicillin (100 μg·mL^{-1}/100 U·mL^{-1}) at conditions of 37 °C in a 95% humidified air atmosphere with 5% CO_2. The HepG2 cells were collected and then washed three times with ice-cold PBS buffer to remove interferences from FBS. Then HepG2 cells were suspended with an appropriate volume of PBS buffer and counted on an automated Cell Counter (Countstar, China). Thereafter, the suspension of cells was diluted by PBS buffer, making 0, 500, 5000, 10000, 20000, 30000 or 40000 cells in 100 μL of suspension. After that, cell lysates were obtained by sonicating for 5 min in ice bath (keep the temperature below 4 °C) and then centrifuged to remove the cell debris at 10,000 rpm at 4 °C for 30 min. In the meantime, the other group was prepared by pretreating with a thio-blocking compound N-ethylmaleimide (NEM, 0.1 mM). The resulting supernatants were used as the final samples and detected as above described.

Analysis of GSH in human serum samples

To assess applicability for detecting GSH in complex real samples, human serum samples were examined in this study. Human whole blood sample (5 mL) was collected in a heparin anticoagulated tube from healthy volunteers. 1 mL of blood sample was centrifuged at 10,000 rpm for 10 min at 4 °C to remove the hemocytes. The supernatant fluid (100 μL) was collected and diluted with 900 μL of 50% methanol/PBS to precipitate protein for 3 min. [29] After centrifugation, the supernatant was collected as 10% deproteinized human plasma. 25 μL of 10% deproteinized human plasma were diluted with 75 μL of ultrapure water or spiked with increasing content of GSH (2, 5, 7.5 μM) for following detection. Finally, the resulting samples were detected as above described process.

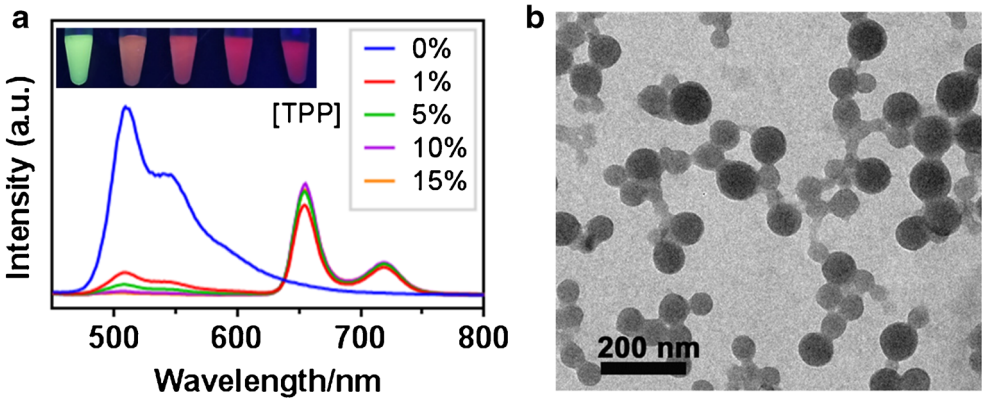

Fig. 2 **a** Fluorescence emission spectrum of P-dots with different TPP dopant ratio vs PEPV (excited at 458 nm), the inset is a photograph corresponding to different feeding ratio (from left to right: 0, 1, 5, 10, 15 wt%) under UV light; (**b**) Representative TEM image of the P-dots

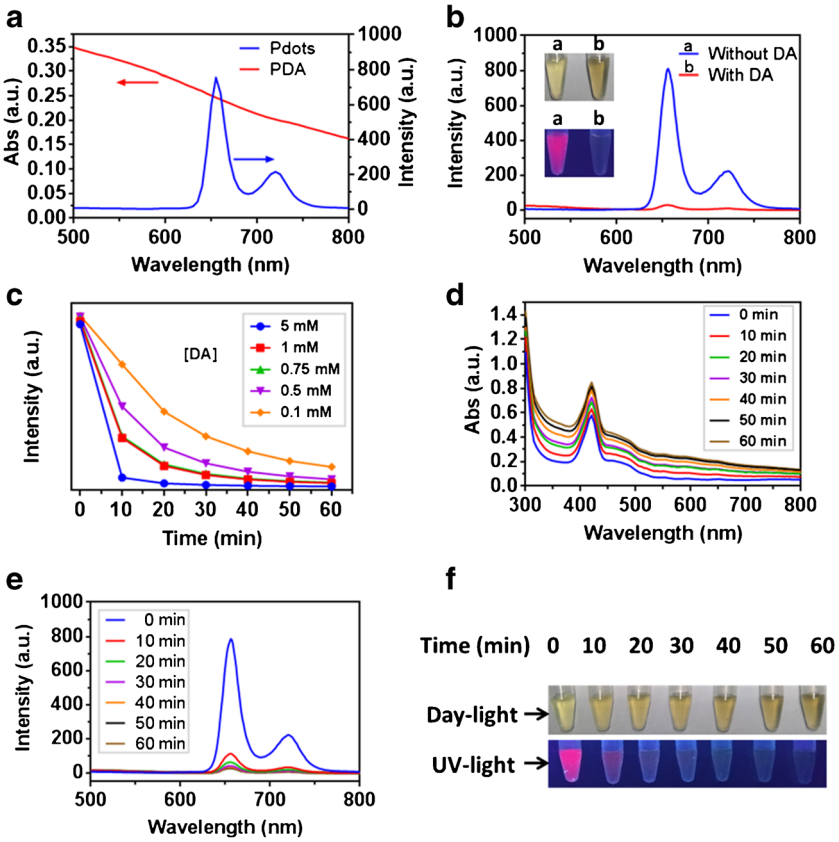

Fig. 3 The optical properties of P-dots with DA. **a** The absorbance of PDA and fluorescence spectra of P-dots (excited at 458 nm); (**b**) The fluorescence spectra of P-dots solution without or with DA (5 mM) in a Tris-HCl buffer (pH 8.5) (excited at 458 nm); (**c**) Plot of the fluorescence intensity change of P-dots solution (emission at 656 nm) response to different concentrations of DA (0.1, 0.5, 0.75, 1 and 5 mM) as a function of time from 0 to 60 min; (**d**) The absorbance spectra of P-dots (0.4 mg·mL^{-1}) and DA (0.75 mM) reaction solution in a Tris-HCl buffer (pH 8.5) from 0 to 60 min; (**e**) The fluorescence spectra of P-dots (0.4 mg·mL^{-1}) and DA (0.75 mM) reaction solution in a Tris-HCl buffer (pH 8.5) from 0 to 60 min (excited at 458 nm); (**f**) Corresponding pictures of (**e**) under day-light and UV-light

The emission at 656 nm was measured and used for calculation. The concentration of GSH in blood sample was calculated using the calibration curve. The sample also detected using DTNB-based assay protocol, see ESM for details.

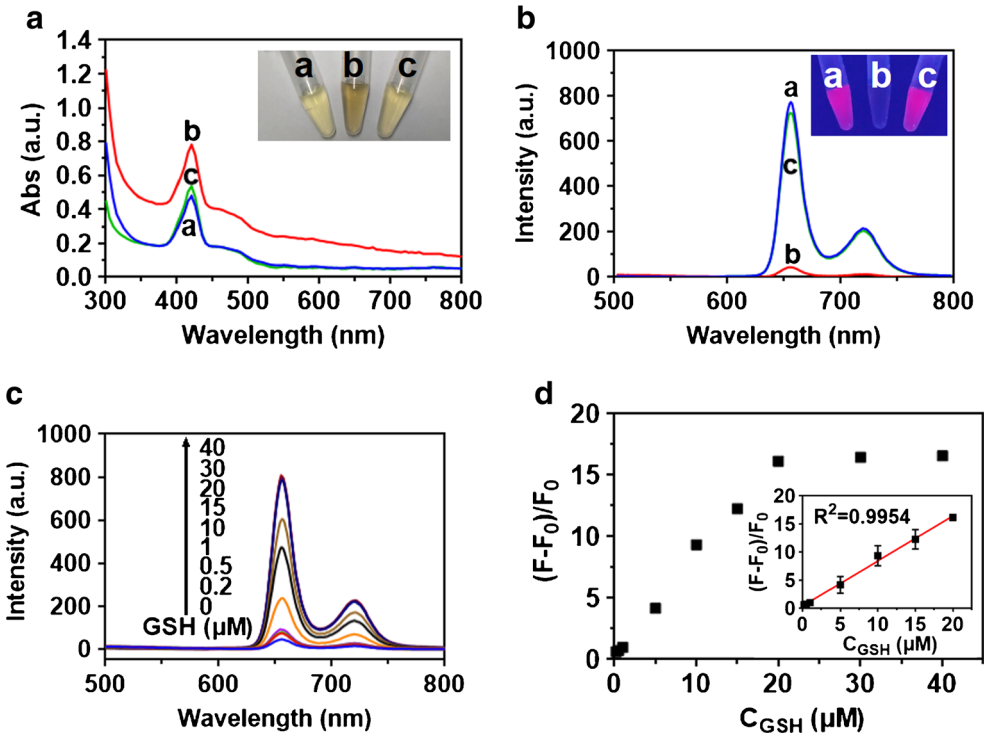

Fig. 4 The optical properties of P-dots and dopamine-melanin nanosystem in GSH detection. **a** The absorbance of P-dots, P-dots/DA, and P-dots/DA/GSH in a Tris-HCl buffer (pH 8.5), respectively; Concentrations: P-dots, 0.4 mg·mL^{-1}; GSH, 50 μM; DA, 0.75 mM; (**b**) Corresponding fluorescence emission spectra (excited at 458 nm) and photographs under UV light of (A); (**c**) The fluorescence intensity change of P-dots/DA solution in response to different concentrations of GSH (0, 0.2, 0.5, 1, 10, 15, 20, 30, 40 μM); (**d**) The relationship between (F-F_0)/F_0 ratio (emission at 656 nm) and GSH concentration. Inset is the linear relationship between (F_0-F)/F_0 and GSH ranging from 0.2 to 20 μM

Table 1 Comparison of methods for GSH determination

Materials	Detection method	Linear range (μM)	Detection limit (μM)	Reference
TMB-MnO_2 nanosheets	Colorimetric method	1–25	0.3	[31]
Acidic potassium permanganate	Chromatography	0.75–100	0.5	[8]
Carbon nanotubes	Electrochemistry	10–60	3.0	[9]
Magnetic-Plasmonic nanocomposite	Surface-enhanced Raman scattering	10^{-6}-10	Not given	[32]
g-C_3N_4–MnO_2 nanocomposites	Fluorescence	0–2000	0.2	[15]
PDs-PDA composites	Fluorescence	0.2–20	0.06	This work

Results and discussion

Synthesis and characterization of polymer dots

To conduct the GSH detection platform, the near-infrared (NIR) fluorescent P-dots used as fluorescent probe were first prepared by nano-precipitation method. The semiconducting polymer PEPV, a non-metallic conducting material wildly used in solar panels, used as the energy donor. TPP, a small molecular dye with a near-infrared emission, used as energy acceptor. After mixing with PSMA, which acted as stabilizing agent, the PEPV and TPP were encapsulated into a nanoparticle by hydrophobic interaction. The NIR fluorescent P-dots enable the detection platform with less scattering in turbid media and reduce interference from the common autofluorescence of biological matrix. To obtain the appropriate feeding ratio of energy donor and acceptor, we varied the TPP concentration to optimize fluorescence properties of P-dots. The overlap of Q band absorption (510 nm) and excitation spectrum of TPP with PEPV emission enable resonance energy transfer from PEPV to TPP (Fig. S1A and 1B). The fluorescence intensity changes in response to different feeding ratio of PEPV versus TPP (Fig. 2a). The abroad emission from 400 to 600 nm attributed to the PEPV polymer. However, after the doping with TPP, the fluorescence emission of PEPV was reduced clearly, the sharp and strong peak of TPP at 656 nm and 725 nm arose. The fluorescence of TPP gradually increased with increasing TPP content ranging from 0 wt% to 10 wt%, and saturated at 10 wt% due to almost all of the energy from PEPV transferred to TPP. Further adding of TPP content did not obviously increase or even reduce the fluorescence for the formation of minor aggregates with aggregation-caused quenching (ACQ) side-effects. Thus, we selected the 10 wt% as the feeding ratio of PEPV versus TPP throughout the following experiments. Additionally, at the of excitation of P-dots, the TPP was excited slightly when compared with that of P-dots (Fig. S1C). The result showed that the fluorescence resonance energy transfer from PEPV to TPP. TEM shows that the P-dots are about 50 nm with nearly spherical and monodispersed morphology (Fig. 2b). The hydrodynamic diameter, ζ-potential and absorption of P-dots confirmed the successfully synthesized of P-dots and can be used as NIR fluorescent probe (Fig. S1D, S2 and S3).

Fluorescence quenching of polymer dots by self-polymerization of dopamine

The spontaneous oxidative polymerization of dopamine can happen under a weak alkaline condition and produced melanin-like PDA coating or nanoparticle. As shown in Fig. 3a, the PDA has a broad and monotonic extended absorbance from the UV-vis to NIR. This overlaps well with the NIR

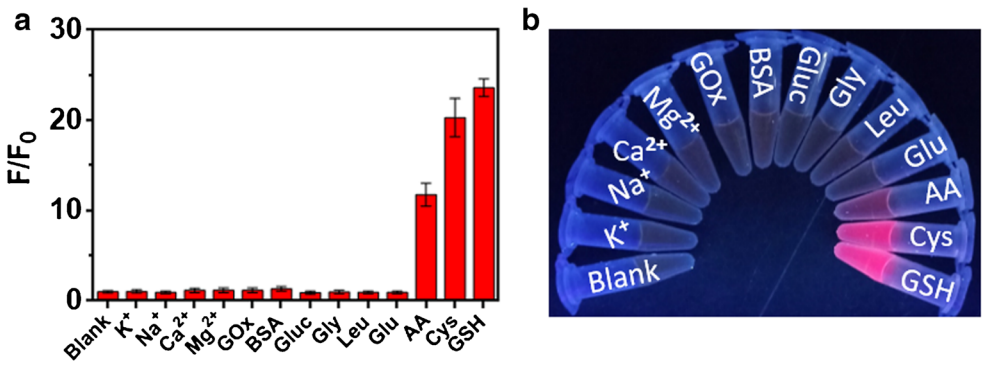

Fig. 5 Selectivity of the P-dots and dopamine-melanin nanosystem for GSH. **a** Relative fluorescence intensity changes of P-dots/DA sensing system in the presence of potential interferences (fluorescence intensity at 656 nm for calculation). **b** Corresponding photographs of (A) under 365 nm UV light illumination. Concentration: KCl, NaCl, $CaCl_2$ and $MgCl_2$: 0.1 mM; GOx, 0.01 mg·mL^{-1}; BSA and Glucose, 1 mg·mL^{-1}; Gly, Leu, Glu, AA, Cys and GSH, 30 μM

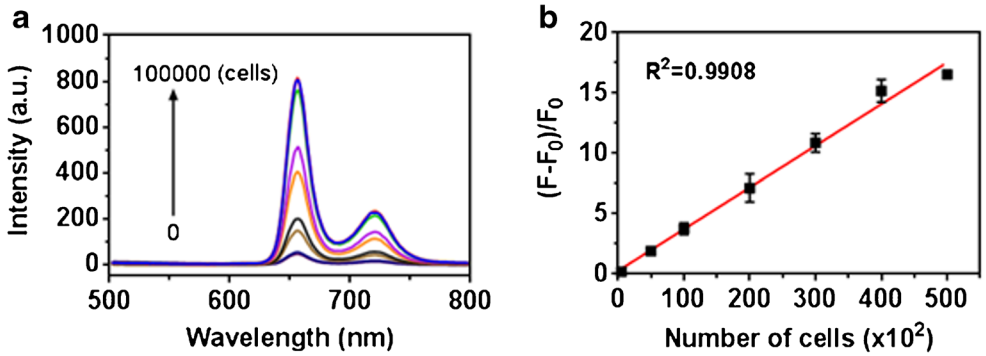

Fig. 6 Intracellular GSH detection. **a** The fluorescence intensity changes of P-dots-DA detection system in response to intracellular GSH generated from various numbers of cells (0, 500, 5000, 10000, 20000, 30000, 40000 and 50000 cells); (**b**) A linear relationship between fluorescence change ratios (F_0-F)/F_0 and number of cells ranging from 0 to 50000 cells. F_0 and F refer to fluorescence intensity (emission at 656 nm) in the before and after treatment of intracellular GSH, respectively

emission of P-dots and enables occur resonance energy transfer. The effect of pH on PDA formation was tested firstly, and the pH of 8.5 can lead the complete fluorescence quenching and was used as reaction condition (Fig. S4). The energy transfer was proved by the observation of remarkably fluorescence quenching of PDA on P-dots under excitation (Fig. 3b). The dopamine-melanin was gradually formed as the function of the reaction time. To obtain a sensitive detection of GSH, the fluorescence intensity change response to different concentrations of DA was optimized. A rapid decrease of the fluorescence intensity was observed between 0.1 and 0.75 mM within 30 min, and slightly changed when the concentration above 0.75 mM (Fig. 3c). Accordingly, 0.75 mM of DA was selected as the optimum concentration. The optimized reaction time was examined by the absorbance and fluorescence intensity change of the P-dots and DA solution towards different reaction time (Fig. 3d, e and f). Although the absorbance of reaction system gradually increased with the reaction time (Fig. 3d), the fluorescence intensity decreasing slightly beyond 30 min as present in Fig. 3e, f. The formation of PDA coating was further verified by TEM examination (Fig. S5). The Stern-Volmer plot is curved (Fig. S6), which indicating that both static and dynamic quenching cause the fluorescence quenching of P-dots in the detection nanosystem.

GSH detection based on P-dots and dopamine-melanin composites

Inspired by the inhibition property of endogenous antioxidants in melanin synthesis, [30] the feasibility of inhibition of spontaneous oxidative polymerization of dopamine by GSH were then tested. As shown in Fig. 4a, the absorbance of P-dots solution increased a lot with addition of DA in a Tris-HCl buffer (pH 8.5), and the corresponding solution turned from light yellow to brown. However, in the presence of GSH, the self-polymerization of dopamine in P-dots solution was inhibited. Its absorbance is similar to that of untreated P-dots solution and maintains light yellow color. The inhibition effect by GSH also revealed by monitoring the fluorescence changes of P-dots at 656 nm (Fig. 4b). In the absence of GSH, the fluorescence emission of P-dots decreased obviously with the formation of dopamine-melanin. However, the valid antiquenching effect was observed when the P-dots solution was pretreated with GSH. Subsequently, the applicability the proposed sensing system for GSH detection in aqueous solutions was examined. As shown in Fig. 4c, the antiquenching effect of P-dots increased gradually as the concentrations of GSH increased from 0 to 20 μM, and thereafter reached a steady state when the concentration of GSH was above 20 μM. The linear relationship of the ($F-F_0$)/F_0 ratio

Table 2 Detection of GSH in human serum samples

Method	Added GSH (μM)	Detected GSH (μM)	Recovery(%)	RSD (n = 3, %)
This method	0	1.01	/	4.30
	2	3.11	103.3	2.07
	5	5.90	98.2	2.43
	7.5	8.28	97.4	1.72
DTNB method	0	1.21	/	3.68
	2	3.25	101.24	3.23
	5	6.22	100.16	2.15
	7.5	8.67	99.54	1.98

versus GSH concentration ($(F-F_0)/F_0 = 0.8006[GSH] + 0.4093$, $R^2 = 0.9954$ ($n = 3$)) was obtained from 0.2 to 20 μM (Fig. 4d), where F and F_0 represent the fluorescence intensity of P-dots at 656 nm in the presence and absence of GSH, respectively. According to the definition of three times the deviation of the blank signal (3σ), the calculated detection limit was 0.06 μM. This comes up to or even better than those previously established methods for GSH detection (Table 1). The NIR fluorescent P-dots can reduce interference from the biological matrix. These results imply that the P-dots and dopamine-melanin composites can be serviced as a potential and promising method for GSH detection.

Selectivity

To investigate the applicability of the detection system for GSH, the selectivity over some potential non-target interferences were measured, such as some metal ions (K^+, Na^+, Ca^{2+}, Mg^{2+}), proteins (GOx, BSA), amino acids (Gly, Leu, Glu) and Glucose. The result indicated that these interference substances did not cause a significant fluorescence response of the system (Fig. 5). Although, the measurable signal changes resulted from AA and Cys were observed in present study, their biological concentrations are much lower than that of GSH. [31, 33, 34] This result clearly demonstrates that this method showed good selectivity for GSH and can be used for real samples.

Determination of intracellular GSH

It is well known that the intracellular GSH plays important role as endogenous antioxidant in biological process and serves many vital cellular functions. [1] Therefore, the detection of GSH level in the biological samples is of great significance. Here, the lysates of HepG2 cells were used as a representative biological sample for intracellular GSH detection. Firstly, the intracellular GSH level of lysates was used to induce fluorescence response of P-dots/DA detection system. As show in Fig. S7, the intracellular GSH caused similar fluorescence response as that of GSH in aqueous solution descripted above. Subsequently, the fluorescence intensity changes of P-dots/DA sensing system in response to different number of HepG2 cells suspensions ranging from 0 to 50000 cells were determined. As present in Fig. 6a, the fluorescence intensity was increased with the number of cells increase from 0 to 50000, and unchanged when the number of cells was above 50000. The calibration plot for intracellular GSH detection was determined as $(F-F_0)/F_0 = 0.0346$[number of cells] + 0.2651 with a good correlation coefficient of 0.9908 ($n = 3$) from 0 to 50000 cells (Fig. 6b). When the lysates samples were pretreated with the thiol-blocking reagent NEM, the antiquenching effect of GSH in lysates for the P-dots-DA sensing system was inhibited (Fig. S8). Hence, this detection system was turned out to be a valid method for the determination of intracellular GSH without being interfered by other intracellular biomolecules.

Assay of GSH in human serum samples

Finally, the GSH in human serum samples was detected to further verify the practicability of P-dots-DA detection system. The human serum was first treated by centrifugation and diluted 40-folds to reduce the potential interference. As show in Table 2, the recoveries with 97.4–103.3% were gained, with relative standard deviations (RSD) from 1.72 to 2.43%, which is acceptable in complex real samples analysis for quantitative assays. The result was agreement with that of 5, 5′-dithiobis-2-nitrobenzoic acid (DTNB)-based method. Therefore, the P-dots-DA detection system can be applied to sensitive and selective analysis of GSH in real samples.

The excitation wavelength at blue visible region (458 nm) may make the probe prone to interferences by biomatter, such as blood, serum, cells etc. Therefore, P-dots with red region excitation and emission can be designed for developing detection system in the future.

Conclusions

We have constructed a sensitive and selective fluorescent detection platform for GSH based on P-dots-dopamine-melanin composites. The dopamine self-polymerization on the surface of P-dots can be inhibited by GSH effectively, and used for detecting GSH sensitively and selectively. Importantly, the system was used to detect intracellular GSH and GSH in human serum samples with favourable results. The excitation wavelength at blue visible region may make the probe prone to interferences by biomatter. To reduce the interferences from biomatter, the P-dots with red region excitation and emission can be designed for developing detection system in the future. Therefore, the proposed detection system demonstrated its great potential to study other chem/bio sensing about GSH in biological and diagnostic applications.

Acknowledgements This work was supported by the National Natural Science Foundation of China (Grant No. 21605021 and 21705022), Joint Funds for the Innovation of Science and Technology of Fujian province (Grant No. 2016Y9060 and 2017Y9115), the Young and Middle-aged Talent Training Project of Fujian Provincial Health and Family Planning Commission (Grant No. 2018-ZQN-75), the China Postdoctoral Science Foundation, the Natural Science Foundation of Fujian Province of China (Grant No. 2016 J05206), the Medical Innovation grant of Fujian province (Grant No. 2018-CX-49) and the Startup Fund of Mengchao Hepatobiliary Hospital of Fujian Medical University (Grant No. QDZJ-2017-004).

Compliance with ethical standards The author(s) declare that they have no competing interests.

References

1. Valko M, Rhodes CJ, Moncol J et al (2006) Free radicals, metals and antioxidants in oxidative stress-induced cancer. Chem Biol Interact 160:1–40. https://doi.org/10.1016/j.cbi.2005.12.009
2. Pastore A, Federici G, Bertini E, Piemonte F (2003) Analysis of glutathione: implication in redox and detoxification. Clin Chim Acta 333:19–39. https://doi.org/10.1016/S0009-8981(03)00200-6
3. Sies H (1999) Glutathione and its role in cellular functions. Free Radic Biol Med 27:916–921. https://doi.org/10.1016/S0891-5849(99)00177-X
4. Dröge W, Breitkreutz R (2000) Glutathione and immune function. Proc Nutr Soc 59:595–600. https://doi.org/10.1017/S0029665100000847
5. Estrela JM, Ortega A, Obrador E (2006) Glutathione in Cancer Biology and Therapy. Crit Rev Clin Lab Sci 43:143–181. https://doi.org/10.1080/10408360500523878
6. Ballatori N, Krance SM, Notenboom S et al (2009) Glutathione dysregulation and the etiology and progression of human diseases. Biol Chem 390:191–214. https://doi.org/10.1515/BC.2009.033
7. Wu G, Fang Y-Z, Yang S et al (2004) Glutathione Metabolism and Its Implications for Health. J Nutr 134:489–492. https://doi.org/10.1093/jn/134.3.489
8. McDermott GP, Francis PS, Holt KJ et al (2011) Determination of intracellular glutathione and glutathione disulfide using high performance liquid chromatography with acidic potassium permanganate chemiluminescence detection. Analyst 136:2578–2585. https://doi.org/10.1039/c1an00004g
9. Lee PT, Goncalves LM, Compton RG (2015) Electrochemical determination of free and total glutathione in human saliva samples. Sensors Actuators B Chem 221:962–968. https://doi.org/10.1016/j.snb.2015.07.050
10. Feng J, Huang P, Shi S et al (2017) Colorimetric detection of glutathione in cells based on peroxidase-like activity of gold nanoclusters: A promising powerful tool for identifying cancer cells. Anal Chim Acta 967:64–69. https://doi.org/10.1016/j.aca.2017.02.025
11. Liu J, Meng L, Fei Z et al (2017) MnO_2 nanosheets as an artificial enzyme to mimic oxidase for rapid and sensitive detection of glutathione. Biosens Bioelectron 90:69–74. https://doi.org/10.1016/j.bios.2016.11.046
12. Xu H-H, Deng H-H, Lin X-Q et al (2017) Colorimetric glutathione assay based on the peroxidase-like activity of a nanocomposite consisting of platinum nanoparticles and graphene oxide. Microchim Acta 184:3945–3951. https://doi.org/10.1007/s00604-017-2429-3
13. Gao W, Liu Z, Qi L et al (2016) Ultrasensitive Glutathione Detection Based on Lucigenin Cathodic Electrochemiluminescence in the Presence of MnO_2 Nanosheets. Anal Chem 88:7654–7659. https://doi.org/10.1021/acs.analchem.6b01491
14. Wei C, Liu X, Gao Y et al (2018) Thiol–Disulfide Exchange Reaction for Cellular Glutathione Detection with Surface-Enhanced Raman Scattering. Anal Chem 90:11333–11339. https://doi.org/10.1021/acs.analchem.8b01974
15. Zhang X-L, Zheng C, Guo S-S et al (2014) Turn-On Fluorescence Sensor for Intracellular Imaging of Glutathione Using g-C_3N_4 Nanosheet–MnO_2 Sandwich Nanocomposite. Anal Chem 86:3426–3434. https://doi.org/10.1021/ac500336f
16. Zhang D, Zheng A, Li J, et al (2017) Tumor microenvironment activable self-assembled DNA hybrids for pH and redox dual-responsive chemotherapy/PDT treatment of hepatocellular carcinoma. Adv Sci 1600460. https://doi.org/10.1002/advs.201600460
17. Yang Y, Zhao Q, Feng W, Li F (2013) Luminescent Chemodosimeters for Bioimaging. Chem Rev 113:192–270. https://doi.org/10.1021/cr2004103
18. Niu L-Y, Guan Y-S, Chen Y-Z et al (2012) BODIPY-Based Ratiometric Fluorescent Sensor for Highly Selective Detection of Glutathione over Cysteine and Homocysteine. J Am Chem Soc 134:18928–18931. https://doi.org/10.1021/ja309079f
19. Liu J, Bao C, Zhong X et al (2010) Highly selective detection of glutathione using a quantum-dot-based OFF-ON fluorescent probe. Chem Commun (Camb) 46:2971–2973. https://doi.org/10.1039/b924299f
20. Tian D, Qian Z, Xia Y, Zhu C (2012) Gold Nanocluster-Based Fluorescent Probes for Near-Infrared and Turn-On Sensing of Glutathione in Living Cells. Langmuir 28:3945–3951. https://doi.org/10.1021/la204380a
21. Zhou L, Lin Y, Huang Z et al (2012) Carbon nanodots as fluorescence probes for rapid, sensitive, and label-free detection of Hg^{2+} and biothiols in complex matrices. Chem Commun 48:1147–1149. https://doi.org/10.1039/C2CC16791C
22. Deng R, Xie X, Vendrell M et al (2011) Intracellular Glutathione Detection Using MnO_2 -Nanosheet-Modified Upconversion Nanoparticles. J Am Chem Soc 133:20168–20171. https://doi.org/10.1021/ja2100774
23. Feng L, Zhu C, Yuan H et al (2013) Conjugated polymer nanoparticles: preparation, properties, functionalization and biological applications. Chem Soc Rev 42:6620–6633. https://doi.org/10.1039/c3cs60036j
24. Wu C, Chiu DT (2013) Highly Fluorescent Semiconducting Polymer Dots for Biology and Medicine. Angew Chem Int Ed 52:3086–3109. https://doi.org/10.1002/anie.201205133
25. Lyu Y, Pu K (2017) Recent Advances of Activatable Molecular Probes Based on Semiconducting Polymer Nanoparticles in Sensing and Imaging. Adv Sci 4:1600481. https://doi.org/10.1002/advs.201600481
26. Guo L, Niu G, Zheng X et al (2017) Single Near-Infrared Emissive Polymer Nanoparticles as Versatile Phototheranostics. Adv Sci 4:1700085. https://doi.org/10.1002/advs.201700085
27. Yin C, Zhen X, Fan Q et al (2017) Degradable Semiconducting Oligomer Amphiphile for Ratiometric Photoacoustic Imaging of Hypochlorite. ACS Nano 11:4174–4182. https://doi.org/10.1021/acsnano.7b01092
28. Sun K, Tang Y, Li Q et al (2016) In Vivo Dynamic Monitoring of Small Molecules with Implantable Polymer-Dot Transducer. ACS Nano 10:6769–6781. https://doi.org/10.1021/acsnano.6b02386
29. Wang D, Chen C, Ke X et al (2015) Bioinspired Near-Infrared-Excited Sensing Platform for in Vitro Antioxidant Capacity Assay Based on Upconversion Nanoparticles and a Dopamine–Melanin Hybrid System. ACS Appl Mater Interfaces 7:3030–3040. https://doi.org/10.1021/am5086269
30. Matsuki M, Watanabe T, Ogasawara A et al (2008) Inhibitory Mechanism of Melanin Synthesis by Glutathione. Yakugaku Zasshi 128:1203–1207. https://doi.org/10.1248/yakushi.128.1203
31. Ahsan H (2011) Arsenic in drinking water. Kaohsiung J Med Sci 27:358–359. https://doi.org/10.1016/j.kjms.2011.05.002
32. Saha A, Jana NR (2013) Detection of Cellular Glutathione and Oxidized Glutathione Using Magnetic–Plasmonic Nanocomposite-Based "Turn-Off" Surface Enhanced Raman Scattering. Anal Chem 85:9221–9228. https://doi.org/10.1021/ac4019457
33. Yu F, Li P, Wang B, Han K (2013) Reversible Near-Infrared Fluorescent Probe Introducing Tellurium to Mimetic Glutathione Peroxidase for Monitoring the Redox Cycles between Peroxynitrite

and Glutathione in Vivo. J Am Chem Soc 135:7674–7680. https://doi.org/10.1021/ja401360a

34. Wang Y, Jiang K, Zhu J et al (2015) A FRET-based carbon dot–MnO_2 nanosheet architecture for glutathione sensing in human whole blood samples. Chem Commun 51:12748–12751. https://doi.org/10.1039/C5CC04905A